

PORE-PRESSURE PREDICTION AND CRITERION OF LIQUEFACTION  
IN SATURATED SANDY SOIL UNDER CYCLIC LOADING

Liu, Ying (I)

SUMMARY

Analytical expressions describing the increments of Residual pore pressure induced by uniform or irregular cyclic loading in saturated sandy soil under undrained condition are presented. In the expressions, the initial stress conditions are considered, and six parameters correlated only with the characteristics of soil are involved. Moreover, the process of liquefaction in the saturated sandy soil is discussed based on the typical records of triaxial test on the soil. The process of liquefaction in saturated sandy soil can be divided into three phases, namely, dynamic instability, static instability, and liquefaction. The equations of shear stress and pore pressure at the beginning of each phase are given.

INTRODUCTION

Increase of pore pressure in saturated sandy soil under undrained earthquake loading condition must be taken into consideration in investigating the aseismic stability and liquefaction potential of saturated sand deposit from the effective stress viewpoint.

In order to conduct this problem, we have done a great deal of cyclic triaxial test. Sand sample used was taken from the Douhe Dam site where sand boils occurred during 1976 Tangshan Earthquake, the physical properties of the soil are shown as follows:

Mean size diameter = 0.2 mm; Uniformity coefficient = 4; Maximum dry unit weight = 1.68  $g_r/cm$ ; Minimum dry unit weight = 1.38  $g_r/cm$ ; Dry unit weight for testing = 1.58  $g_r/cm$ .

Specimens were consolidated under given consolidation ratios, then cyclic loading were applied in axial direction up to a level, at which failure appeared under undrained condition.

RESIDUAL PORE PRESSURE IN SATURATED  
SANDY SOIL UNDER CYCLIC LOADING

In the Case of Uniform Cyclic Loading

The increment in residual pore pressure per cycle was defined as the difference between the pore pressure at the end of one cycle and the one at the end of the successive cycle. So the increment in residual pore pressure during the  $N$ th cycle can be expressed by equation (1)

$$\Delta U_N = U_N - U_{N-1} \quad (1)$$

---

(I) Associate Professor, Institute of Engineering Mechanics (IEM),  
Academia Sinica, Harbin, China

Consequently, the residual pore pressure at the Nth cycle can be expressed by equation (2)

$$U_N = U_{N-1} + \Delta U_N \quad (2)$$

where,  $\Delta U_N$  = the increment in pore pressure during the Nth cycle;  $U_N$  = the residual pore pressure at the Nth cycle; and  $U_{N-1}$  = the residual pore pressure at the (N-1)th cycle.

After normalizing each term in equation (2) by the mean stress  $\sigma_0 = \frac{1}{3}(\sigma_1 + 2\sigma_c)$ , the normalized increment in residual pore pressure  $\Delta U_N^*$  during the Nth cycle can be expressed by equation (3)

$$\Delta U_N^* = U_N^* - U_{N-1}^* \quad (3)$$

Based on the test data, a relationship between the residual pore pressure ratio  $\Delta U_N^*/(1 - U_{N-1}^*)$  and the applied stress ratio  $\sigma_a^*/(1 - U_{N-1}^*)$  was obtained as shown in Fig. 1.

It can be seen from Fig. 1 that the test data can be fitted by a group of straight lines in the log-log scale paper parallel to each other; besides, the interceptions of these lines on the ordinate are different for different cycles, so the following equation can be obtained.

$$\frac{\Delta U_N^*}{1 - U_{N-1}^*} = F(N) \left( \frac{|\sigma_a^*|}{1 - U_{N-1}^*} \right)^{\alpha_1} \quad (4)$$

Consequently

$$F(N) = \frac{\Delta U_N^*}{1 - U_{N-1}^*} / \left( \frac{|\sigma_a^*|}{1 - U_{N-1}^*} \right)^{\alpha_1} \quad (5)$$

Based on the test data shown in Fig. 2, a concrete form of  $F(N)$  can be obtained as follows

$$F(N) = \frac{\gamma_1}{N^{\beta_1}} \quad (6)$$

Combining equation (4) and equation (6) the equation for predicting the increment of pore pressure during any cycle can be obtained as follows

$$\Delta U_N^* = (1 - U_{N-1}^*) \frac{\gamma_1}{N^{\beta_1}} \left( \frac{|\sigma_a^*|}{1 - U_{N-1}^*} \right)^{\alpha_1} \quad (7)$$

therefore, the normalized residual pore pressure at Nth cycle can be predicted by the following equation

$$U_N^* = U_{N-1}^* + \Delta U_N^* \quad (8)$$

Clearly, equation (7) is quite similar to that given by Ishibasi et al. (Refs. 1 and 2) previously. But either equation (7) or that given by Ishibasi et al., can be applied to a particular stress condition ( $K_c = 1$  or  $K_c$  condition) only, both are not suitable for the general case.

It can be seen from Fig. 3 that there are some relationships between  $\alpha$ ,  $\beta$  and  $\gamma$  parameters and the consolidation ratios  $K_c$  as shown below (Ref. 3).

$$\alpha = \alpha_1 K_c^{-c_1} \quad (9)$$

$$\beta = \beta_1 K_c^{-c_2} \quad (10)$$

$$\gamma = \gamma_1 K_c^{-c_3} \quad (11)$$

Instead of parameters  $\alpha_1$ ,  $\beta_1$ , and  $\gamma_1$ , substituting  $\alpha$ ,  $\beta$  and  $\gamma$  into equation (7) the general equation for predicting increment in residual pore pressure can be obtained as follows

$$\Delta U_N^* = (1 - U_{N-1}^*) \frac{\gamma}{N^\beta} \left( \frac{|\sigma_{\sigma d}^*|}{1 - U_{N-1}^*} \right)^\alpha \quad (12)$$

Under non-uniform cyclic loading the increment in pore pressure at positive half-cycle is not the same as that at the negative half-cycle. Therefore in such case, the increment in residual pore pressure was defined as the difference between the pore pressure at the end of the first half-cycle and that at the end of the successive half-cycle, so the increment in residual pore pressure during any half-cycle can be predicted by equation (13)

$$\Delta U_R^* = U_R^* - U_{R-1}^* \quad (13)$$

Where,  $R$  = number of half-cycle. In this case, the number of half-cycle must be twice as many as the number of whole cycle  $N$ . Therefore, the function  $F(R)$  which represents the effect of the number of half-cycle was developed. For example, remove the ordinate in Fig. 2 to left-hand a half logarithmic period and take its abscissa as the starting point of the  $\log R$ , then extend the straight line to cross the ordinate at point  $\gamma_i^*$  as shown in Fig. 4.

So, a relationship between the parameter  $\gamma_i^*$  determined under non-uniform cyclic loading and that determined under uniform cyclic loading ( $K_c = 1$ ) can be obtained as follows

$$\gamma_i^* = 2^{\beta_1} \gamma_1 \quad (14)$$

for general case

$$\gamma^* = 2^{\beta} \gamma \quad (15)$$

Therefore, the equation for predicting the residual pore pressure under non-uniform cyclic loading can be obtained as follows

$$\Delta U_R^* = (1 - U_{R-1}^*) \frac{\gamma^*}{R^\beta} \left( \frac{|\sigma_{\sigma d}^*|}{1 - U_{R-1}^*} \right)^\alpha \quad (16)$$

$$U_R^* = U_{R-1}^* + \Delta U_R^* \quad (17)$$

LIQUEFACTION FAILURE OF SATURATED  
SANDY SOIL UNDER CYCLIC LOADING

Critical Equilibrium Condition

In order to study the critical equilibrium condition and the liquefaction failure process of saturated sandy soil under cyclic loading, cyclic triaxial test and data analysis were carried out (Ref. 4). Assuming that under undrained cyclic loading condition, the shear strength of saturated sand consists of two parts, namely, viscous resistance and frictional resistance, the former being directly proportional to the dynamic deformation rate, while the latter being directly proportional to the normal stress. Therefore, the critical equilibrium condition can be written as follows

$$\tau_{dN} = c_{VN} + \sigma'_{dN} \text{tg} \varphi'_d \quad (18)$$

where  $\tau_{dN}$  = shear stress on the failure plane in the Nth cycle (including static stress, too);  $c_{VN}$  = viscous resistance in the Nth cycle;  $\sigma'_{dN}$  = effective normal stress on the failure plane in the Nth cycle (including static normal stress, too);  $\varphi'_d$  = dynamic friction angle.

Referring to Fig. 5, the following equations can be deduced based on our assumption

$$c_{VN} = \xi \frac{\Delta h}{\Delta t} = \frac{1}{2 \cos \varphi'_d} [(\sigma_1' - \sigma_3') - (\sigma_1' + \sigma_3') \sin \varphi'_d] \quad (19)$$

$$\sigma'_{dN} = \sigma_{dN} - u_N = \frac{1}{2} [(\sigma_1' + \sigma_3') - (\sigma_1' - \sigma_3') \sin \varphi'_d] \quad (20)$$

where  $\xi$  = apparent coefficient of viscosity;  $\frac{\Delta h}{\Delta t}$  = average dynamic deformation rate at the Nth cycle;  $\sigma_{dN}$  = total normal stress on the failure plane at the Nth cycle;  $U_N$  = pore pressure at the Nth cycle (see equation (23)).

$\varphi'_d$  in equations (19) and (20) is still unknown at present. On the assumption that, after reaching the critical equilibrium state, the apparent coefficient of viscosity and the dynamic friction angle both remain constant an expression for  $\varphi'_d$  can be established by solving the equations in the two successive cycles. Therefore, from Fig. 5 the following equations can be obtained.

$$\text{tg} \varphi'_d = \frac{\frac{1}{2}(\sigma_1' - \sigma_3') \cos \varphi'_d - c_{VN}}{\frac{1}{2}(\sigma_1' + \sigma_3') - \frac{1}{2}(\sigma_1' - \sigma_3') \sin \varphi'_d} \quad (21)$$

in which the subscript 1 or 2 indicates the given variable belonging to the previous cycle or the later cycle. Substituting the value of  $\varphi'_d$  obtained from equation (21) into equations (19), (20) and (23),  $c_{VN}$  and  $\sigma'_{dN}$  can be determined and hence, the critical equilibrium condition of the saturated sandy soil in this particular case can be obtained.

Process of Liquefaction Failure

A liquefaction test record for the given saturated sand specimen is shown in Fig. 6. After consolidating under  $\sigma_{sc} = 1.0 \text{ Kg/cm}$  and  $\sigma_{1c} = 2.0 \text{ Kg/cm}$ , cyclic load of  $0.53 \text{ Kg/cm}$  was applied to the specimen axially with frequency of one circle per second. Under this anisotropic consolidation condition, liquefaction failure can take place only in the half compression cycle. In this case  $U_N = U_{Nc}$ ,  $\sigma_1' = \sigma_{1c} + \sigma_{ad} - U_{Nc}$ , and  $\sigma_3' = \sigma_{3c} - U_{Nc}$ . Substituting these values into equation (21) the following expression will result

$$\varphi'_d = \sin^{-1} \left[ \frac{\frac{\Delta h_2}{\Delta t} (\sigma_{1c} - \sigma_{3c} + \sigma_{ad})_1 - \frac{\Delta h_1}{\Delta t} (\sigma_{1c} - \sigma_{3c} + \sigma_{ad})_2}{\frac{\Delta h_2}{\Delta t} (\sigma_{1c} + \sigma_{3c} + \sigma_{ad} - 2u_{Nc})_1 - \frac{\Delta h_1}{\Delta t} (\sigma_{1c} + \sigma_{3c} + \sigma_{ad} - 2u_{Nc})_2} \right] \quad (22)$$

The liquefaction test record shown in Fig. 6 is analyzed using equation (22), results of which are shown in Fig. 7.

According to the above mentioned results of test, the liquefaction failure process can be separated into three stages:

(1) Dynamic instability stage

It can be seen from Fig. 5 that, if the pore pressure in the  $N$ th cycle has increased so that the saturated sand specimen begins to reach the critical equilibrium condition, then the expression for pore pressure at that time can be established as follows

$$u_{Nc} = \frac{1}{2 \sin \varphi'_d} [(\sigma_{1c} + \sigma_{ad} + \sigma_{3c}) \sin \varphi'_d - (\sigma_{1c} + \sigma_{ad} - \sigma_{3c}) + 2c_{VN} \cos \varphi'_d] \quad (23)$$

For practical purposes, the static friction angle may be used instead of dynamic friction angle in equation (23), and therefore it can be further simplified as follows

$$u^*_{Nc} = \frac{1}{2 \sin \varphi'_s} [(K_c + K_d) (\sin \varphi'_s - 1) + (\sin \varphi'_s + 1)] \quad (24)$$

in which

$$u^*_{Nc} = \frac{u_{Nc}}{\sigma_{3c}}; \quad K_c = \frac{\sigma_{1c}}{\sigma_{3c}}; \quad K_d = \frac{\sigma_{ad}}{\sigma_{3c}}$$

(2) Static instability stage

It can be seen also that if the pore pressure in the  $N$ th cycle has increased so that the saturated sand specimen begins to reach the static critical equilibrium condition, then the expression for pore pressure at that time can be established as follows

$$u^*_{Nc} = \frac{1}{2 \sin \varphi'_s} [K_c (\sin \varphi'_s - 1) + (\sin \varphi'_s + 1)] \quad (25)$$

(3) Initial liquefaction

It can be seen from Fig. 8 and equation (25) that the pore pressure ratio  $U_{Nc}^* = 1$  i.e., the pore pressure is equal to the confining pressure, it is true only when the static instability is attained under the case  $K_c = 1$ , noting that when  $K_c > 1.0$ , pore pressure  $U_{Nc}$  hasn't attained the level of confining pressure. Therefore, the process of sand liquefaction can not be simulated completely if the consolidation ratio is maintained a constant larger than 1.0.

REFERENCES

- (1) Ishibasi, I, Sherif, M. A. and Tsuchiya, C., 1977, "Pore Pressure Rise Mechanism and Soil Liquefaction", Soils and Foundations, Japanese

Society of Soil Mechanics and Foundation Engineering, Vol. 17, No. 2.

- (2) Sherif, M. A., Ishibasi, I. and Tsuchiya, C., 1978, "Pore-Pressure Prediction during Earthquake Loading", Soil and Foundations, JSSMF, Vol. 18, No. 4.
- (3) Liu Ying, Tong Jun and Qi Xin, 1981, "Residual Pore Pressure in Saturated Sand under Cyclic Loading", China Civil Engineering Journal, China Civil Engineering Society, Vol. 14, No. 3.
- (4) Liu Ying, Tong Jun and Qi Xin, 1981, "Liquefaction Failure of Saturated Sandy Soil under Cyclic Loading", Proceeding of the Joint US-PRC Microzonation Workshop, pp. 71-76.
- (5) Liu Ying, Zhu Li and Tong Jun, 1978, "Dynamic analysis of Sand Layer Underlying the Dou River Earth Dam", Research Report of Institute of Engineering Mechanics, Academia Sinica, No. 78-020.

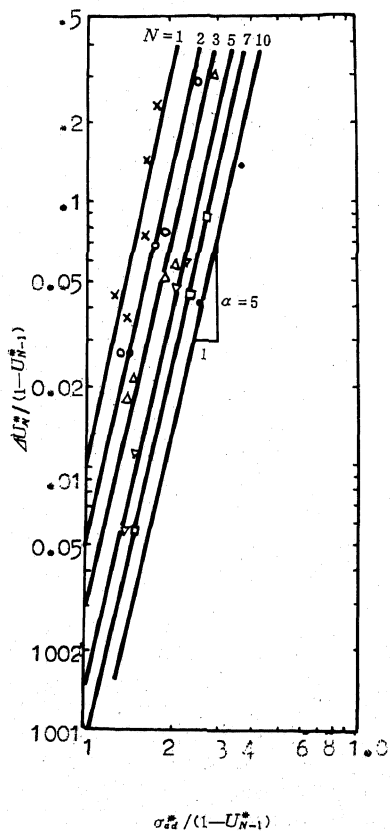


Fig. 1. Pore pressure rise per cycle

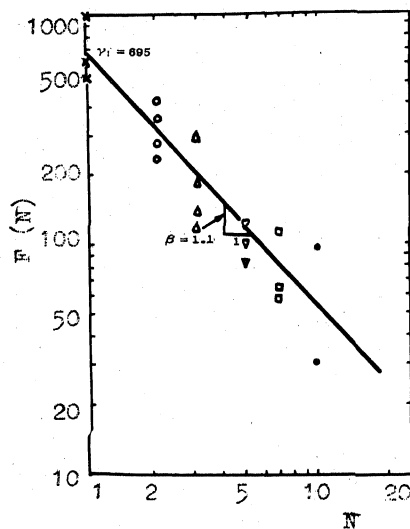


Fig. 2. Function  $F(N)$  versus number of cycle  $N$

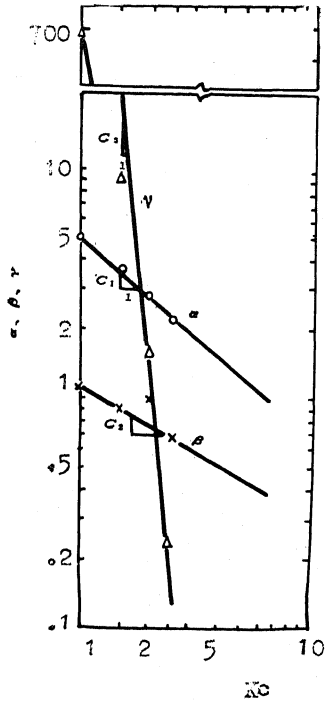


Fig. 3. Parameters  $\alpha$ ,  $\beta$  and  $\gamma$  versus consolidation ratio  $K_c$

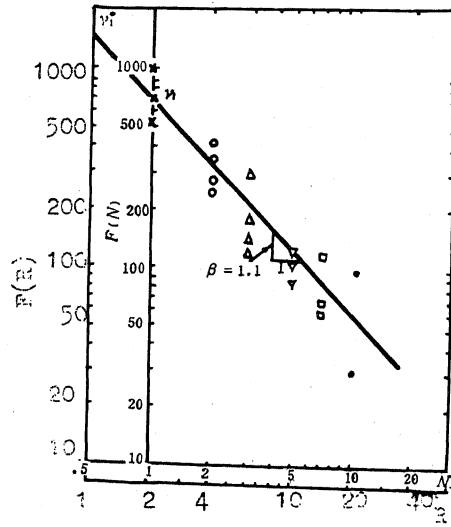


Fig. 4. Function  $F(R)$  versus number of half-cycle  $R$

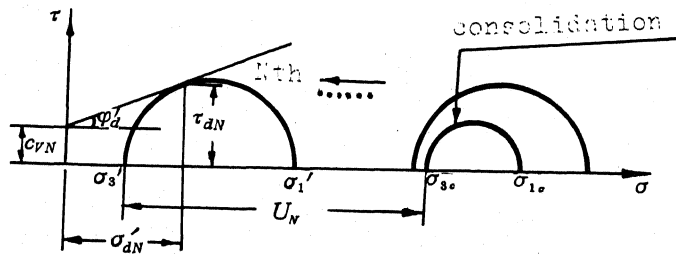


Fig. 5. Critical equilibrium condition in the  $N$ th cycle

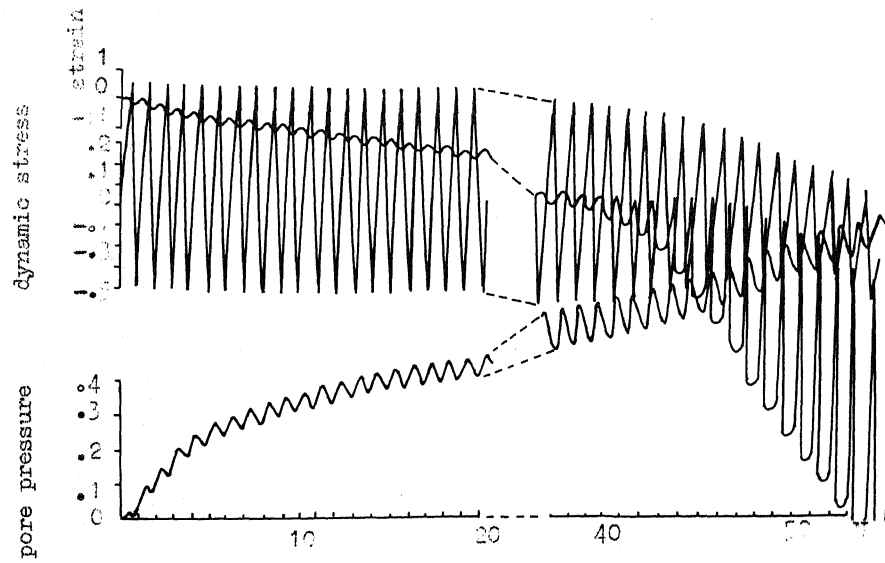


Fig. 6. Typical record of liquefaction test ( $K_c=2$ )

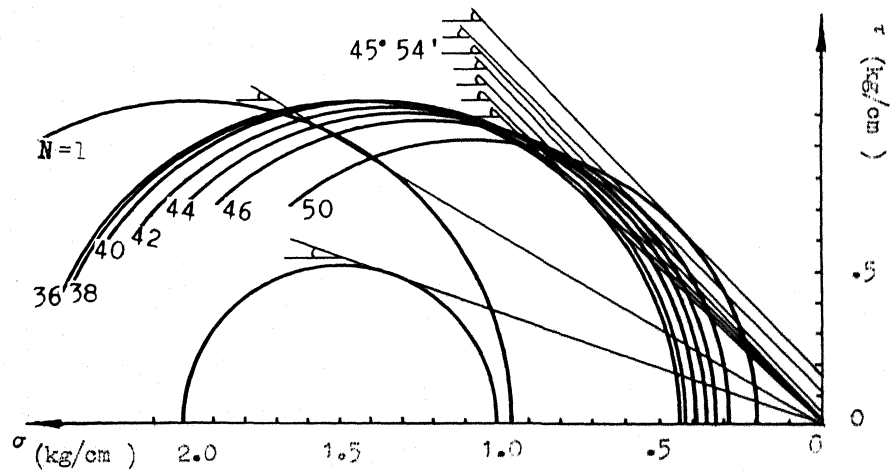


Fig. 7 Mohr's circles under cyclic loading ( $K_c=2$ )

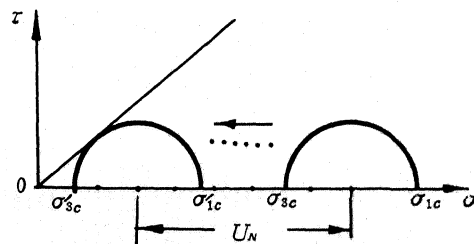


Fig. 8. Static instability condition